

ARTICLE

Steel fiber reinforced RC beams in pure torsion—Load-bearing behavior and modified space truss model

Vincent Oettel 

Institute of Concrete Construction (IfMa),
Leibniz Universität Hannover, Hannover,
Germany

Correspondence

Vincent Oettel, Institute of Concrete
Construction (IfMa), Leibniz Universität
Hannover, Appelstraße 9A, 30167
Hannover, Germany.
Email: oettel@ifma.uni-hannover.de

Abstract

Investigations on steel fiber reinforced concrete (RC) beams in torsion show, that the steel fibers positively influence the torsional load-bearing behavior. Since a systematic evaluation of the previously known test results and the derivation of a generally valid design model were lacking until recently, current codes such as Model Code 2010 do not contain any design models for the consideration of the steel fiber load-bearing effect in the torsion design. Due to this, the existing torsion tests on steel fiber RC were summarized in a database. Furthermore, on the basis of the test results and observations, the space truss model developed by Rausch and later refined by Lampert and Thürlimann, among others, was further developed and supplemented by additional longitudinal and transverse steel fiber tension struts. This modified space truss model was validated with the database and shows good to very good predictions to the torsion test data.

KEYWORDS

concrete, database, RC beam, space truss model, steel fiber, torsion

1 | INTRODUCTION

The torsional behavior of concrete beams, reinforced concrete (RC) beams and, partly, prestressed concrete beams reinforced with steel fibers has been subject to international research since the 1970s. Those experimental results have shown that the cracking torque, the torsional stiffness after cracking and the ultimate torque are positively influenced by steel fibers. To some extent, calculation

equations have been proposed on the basis of the results. These calculation equations are based on different theories or models (elasticity theory, plasticity theory, truss model etc.) and were only slightly modified in some parts, for example, by means of empirical adjustment factors. In addition, these empirical adjustment factors were derived almost exclusively on the basis of the respective authors' own test results, which means that they are only based on a limited number of test results and consequently have only limited validity. A summary and explanation of the different approaches can be found in Reference.¹

However, until recently, neither a systematic evaluation of the existing experimental results published in the literature nor a derivation of a general calculation

Discussion on this paper must be submitted within two months of the print publication. The discussion will then be published in print, along with the authors' closure, if any, approximately nine months after the print publication.

This is an open access article under the terms of the [Creative Commons Attribution-NonCommercial-NoDerivs](https://creativecommons.org/licenses/by-nc-nd/4.0/) License, which permits use and distribution in any medium, provided the original work is properly cited, the use is non-commercial and no modifications or adaptations are made.

© 2022 The Authors. *Structural Concrete* published by John Wiley & Sons Ltd on behalf of International Federation for Structural Concrete.

approach has been carried out. Therefore, equations that take the load-bearing behavior of the steel fiber in torsion design into account are missing in the current design codes and guidelines. For example, the Model Code 2010² (MC2010) does not contain a design model or design equations. However, the MC2010 allows fiber RC beams without longitudinal and transverse reinforcement to be designed, if fiber RC with a hardening tensile behavior is used and the principal tensile stress must not exceed the design value of the ultimate residual tensile strength of the fiber RC (elasticity theory).

Based on this fact, the experimental results of steel fiber reinforced beams under torsion—which can be found in literature—have been summarized in a database, a modified space truss model for the realistic determination of the load-bearing behavior of steel fiber reinforced beams in pure torsion has been developed and validated with the help of the database, which is reported on in References.^{1,3,4} This developed model has been included in Germany in the revised guideline “Steel Fibre Reinforced Concrete” of the German Committee for Reinforced Concrete (DAfStb), which supplements DIN EN 1992-1-1/NAD^{5,6} (EC2/NAD) with specific design rules for steel fiber RC (see Reference^{7,8}). In the meantime, similar models have been developed by References,^{9,10} for example, and compared and validated with a large number of torsion tests in literature.

In the course of this article, it will be examined in the following, whether the approach according to Reference¹ is also compatible with the Model Code 2010, since the torsion design (of RC beams) differs slightly between EC2/NAD and MC2010 and the two codes DAfStb and MC2010 apply, among other things, different residual tensile strengths of the fiber RC (unnotched four-point bending tests vs. notched three-point bending tests, see also Reference¹¹). Before that, however, the torsional behavior of steel fiber RC beams without and with additional steel rebars will be explained. A distinction will be made between pure concrete (C), reinforced concrete (RC), prestressed concrete (PC), steel fiber reinforced concrete (SFRC), steel fiber reinforced concrete reinforced with additional rebars (SFR-RC), and steel fiber reinforced prestressed concrete (SFR-PC).

2 | TORSIONAL LOAD-BEARING BEHAVIOR OF STEEL FIBER REINFORCED BEAMS

2.1 | General

The torsional load-bearing behavior of steel fiber RC was first investigated in the 1970s by Hafeez Khan et al.¹² and Narayanan and Toorani-Goloosalar.¹³ While these tests

had still been limited to SFRC beams, further series of tests were carried out by various researchers in the following years, in which SFR-RC and SFR-PC beams were also investigated in addition to SFRC beams. Some of these investigations aimed to replace the longitudinal and/or transverse reinforcement by steel fibers (see Reference¹⁴) or to design SFR-PC beams without any conventional reinforcement (see Reference¹⁵).

The tests on SFRC and SFR-RC beams showed that, similar to pure concrete (C) and RC beams (see Reference¹⁶), they behaved approximately linear-elastic and the torsional stiffness was not significantly influenced by the steel fibers for non-cracked sections (e.g., References^{17,18}). Moreover, even in the case of SFRC and SFR-RC beams with rectangular cross-section, the initial crack always occurred on the longer cross-section side (h) and at this point inclined centrally at 45° to the beam axis in accordance with the shear stress curve according to elasticity theory (e.g., References^{19,20}). However, by increasing the dosage of the steel fibers, a smaller rising in the torsional cracking moment could be observed, whereas the tensile strength of the applied fiber RC increased at the same time (e.g., Reference²¹). In case of cracked sections, the steel fibers had a significant impact on the load-bearing and deformation behavior of SFRC as well as SFR-RC beams as will be explained below.

2.2 | Steel fiber RC beams without longitudinal and transverse reinforcement

The tests results on SFRC beams show that, either the beams could not be stressed at all or they could only be stressed slightly beyond the torsional cracking moment, depending on the dosage of the fibers and the performance of the fibers.^{18–22} When the torsional cracking load was reached, a crack was formed at an angle of 45° to the longitudinal axis of the beam over 2/3 of the beam circumference, analogue to pure concrete beams (cf. Reference²³), and the remaining cross-section subsequently cracked in the opposite direction due to bending stress (e.g., Reference¹⁹). If the performance of the fibers was high, some additional fine cracks could be observed, but these were not decisive for the failure (e.g., References^{21,22}). Comparable to pure concrete beams (cf. Reference²³), the SFRC beams with low dosages of fibers failed abruptly and broke in two. In contrast to that, robust failure occurred with a high dosage of fibers and the beams did not break in two (e.g., References^{18,20}). Depending on the dosage of fibers and the performance of the fibers, post-failure load-bearing capacity due to fiber pull-out could also be recorded after the ultimate load was reached (e.g., References^{19,21,22}).

Figure 1 shows an example of the torque-twist response of the beams P1, P3, and P6 tested by Craig

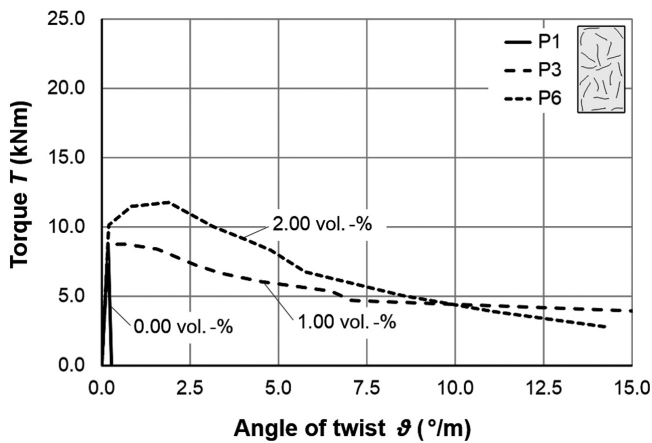


FIGURE 1 Torque-twist response of the beams P1, P3, and P6 reinforced with different dosages of steel fibers according to Reference²¹

et al.²¹ under pure torsion and reinforced with different dosages of steel fibers (0.00 vol.-%, 1.00 vol.-%, and 2.00 vol.-%), but with the same fiber type.

As can be seen, the beam P1 without steel fibers fails abruptly upon reaching the torsional cracking load. In contrast to that, the failure of the fiber reinforced beams P3 and P6 is more robust, whereby P6 with the highest dosage of fibers has a minimally higher cracking moment (about 16%) and can still be stressed slightly (about 16%) after reaching the torsional cracking load with an increase in twisting. Furthermore, the post-cracking load capacity caused by the steel fibers can be clearly seen in beams P3 and P6.

2.3 | Steel fiber RC beams with longitudinal or transverse reinforcement

Experimental investigations on fiber RC beams that were additionally reinforced with longitudinal or transverse reinforcement showed that, analogue to concrete beams with only longitudinal or transverse reinforcement (see Reference²³), a helical crack formed around the cross-section after the torsional cracking load was reached. With a high dosage of fibers, further cracks were observed in some cases, which were not evenly distributed over the beams (e.g., References^{14,17,24}). Similar to pure concrete beams with only longitudinal or transverse reinforcement, failure occurred with a low dosage of fibers when the torsional cracking load was reached or shortly thereafter. With increasing the dosage of fibers, the torsional load could be maintained and in some cases it could even be slightly increased and subsequently maintained (e.g., References^{17,19,24,25}). With increasing twist, these beams failed due to fiber pull-out. Regardless of the dosage of the fibers, the beams did not break in two, as they were

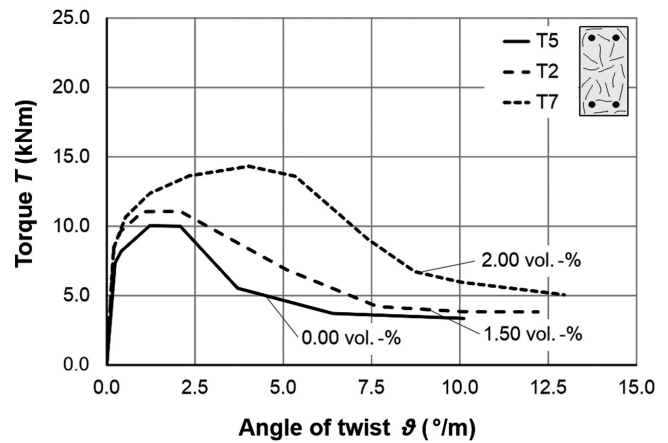


FIGURE 2 Torque-twist response of the beams T5, T2, and T7 reinforced with identical longitudinal reinforcement and different dosages of steel fibers according to References¹⁷

held together by the longitudinal reinforcement and sometimes also by the steel fibers (e.g., Reference¹⁸).

Figure 2 shows an example of the torsional load-bearing behavior of three beams tested under pure torsion, which were reinforced with identical longitudinal reinforcement and different dosages of steel fibers (0.00 vol.-%, 1.50 vol.-%, and 2.00 vol.-%). These are the tests T5, T2, and T7 carried out by Craig et al.,¹⁷ which correspond to the test specimens of Figure 1 in their dimensions and the type of fiber used.

Figure 2 shows that the beam T5 without steel fibers can still support a small load when the crack load is reached and then can hold this load for a short time before it fails. A similar behavior is shown by test specimen T2 with 1.50% by volume steel fibers, whereby an approximately 10% higher load can be supported. In contrast, test specimen T7, with a dosage of steel fibers of 2.50 vol.-%, can support a load that is approximately 40% higher than that of T5 after cracking with an increase in twisting.

It becomes evident from the investigations on fiber RC beams with longitudinal reinforcement according to Mansur and Lim¹⁹ (which are the only ones to provide information on the measured strain of the longitudinal reinforcement), that the longitudinal reinforcement cannot be fully utilized. This also explains the low ultimate torsional loads of the beams, as the failure is always caused by the weaker reinforcement, if so the steel fibers. No equilibrium can be reached in the torsional crack, which causes a premature failure with the formation of a shear fracture. Compared to SFRC beams, the longitudinal reinforcement inhibits crack expansion directly after crack initiation, which means that the torsional cracking moment can be maintained or can even slightly be increased with an increase in twisting. Since the crack widths increase with increasing twisting and the steel fibers are (gradually) pulled out of the concrete, the

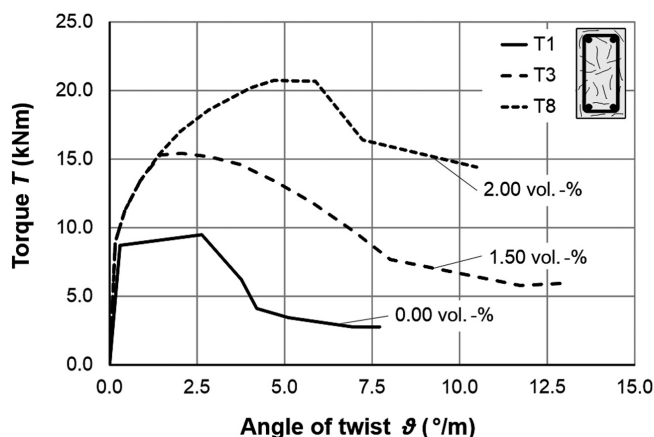


FIGURE 3 Torque-twist response of the beams T1, T3, and T8 reinforced with identical longitudinal and transverse reinforcement and different dosages of steel fibers according to Reference¹⁷

capacity of the steel fibers is exhausted relatively quickly and the supportable torsional moment decreases. Investigations according to Yang et al.²⁴ also show that increasing in the degree of longitudinal reinforcement does not increase the torsional load, but only a higher twist can be applied. Consequently, only the dosage of the fibers has an influence on the ultimate torsional moment. This is similar to fiber RC beams that were reinforced exclusively with transverse reinforcement (e.g., Reference²⁶).

2.4 | Steel fiber reinforced beams with longitudinal and transverse reinforcement

The tests on SFR-RC beams showed that, corresponding to the RC beams under pure torsional loading (see Reference¹⁶), the load could be further increased after the torsional cracking load had been exceeded, and several almost helically running cracks inclined at 45° were formed. Increasing the dosage of fibers led to smaller crack widths and crack spacing and to a larger number of cracks (finer crack pattern) (e.g., References^{18,24,27}). Comparable to RC beams, the torque-twist response principally consists of three distinct phases, namely pre-cracking phase, post-cracking phase and the phase with the yielding of the reinforcement (e.g., References^{27,28}). It was observed that, analogue to RC beams, with a high degree of reinforcement (see Reference¹⁶), the transition phase from pre-cracking phase to post-cracking phase was no longer quite as abrupt or without a sudden increase in twisting by increasing the dosage of the fibers (e.g., References^{24,29}). Furthermore, by increasing the dosage of fibers, a partly significant raise of the torsional failure moment, a higher torsional stiffness in the post-cracking phase and a higher twist were recorded

(e.g., References^{17,24,29}). The failure occurred as a result of a combination of fiber pull-out and tearing of the reinforcement bars.

Figure 3 shows an example of the torque-twist response of the beams T1, T3, and T8 tested by Craig et al.¹⁷ under pure torsion, which were reinforced with identical longitudinal and transverse reinforcement, but different dosages of steel fibers (0.00 vol.-%, 1.50 vol.-%, and 2.00 vol.-%). These test specimens correspond to the tests T5, T2, and T7 according to Figures 1 and 2 with regard to dimensions, the fiber types, the dosages of fibers and the degree of longitudinal reinforcement and differ only in the transverse reinforcement used.

The test specimen T1 without steel fibers can be subjected to slightly higher loads after reaching the torsional cracking load under excessive increase of the twisting and it subsequently fails. The transverse reinforcement for this test specimen was designed in such a way that slightly more than the torsional cracking load could be absorbed (\approx minimum transverse reinforcement) and the transverse reinforcement failed after the abrupt transition from pre-cracking phase to post-cracking phase. Regarding test specimen T3 with 1.50 vol.-% steel fibers, the transition to post-cracking phase is not associated with excessive twisting. Furthermore, a higher torsional stiffness and a more than 62% higher torsional failure moment can be observed. Test specimen T8 with 2.00 vol.-% steel fibers behaves similar, whereby a more than 118% higher torsional load and a higher twisting can be applied.

3 | APPROACHES FOR STEEL FIBER REINFORCED RC BEAMS UNDER TORSION

3.1 | General

From the load-bearing behavior of beams reinforced with steel fibers under pure torsion presented in Section 2 (see Figure 1 to Figure 3), it becomes clear that a significant improvement of the torque-twist response can only be achieved for beams that have been reinforced with longitudinal and transverse reinforcement in addition to the steel fibers (SFR-RC beams). For this reason, an approach for these SFR-RC beams is developed subsequently. As this is based on the space truss model for RC beams, this theory will be briefly described first.

3.2 | Space truss model for RC beams

The space truss theory is the most frequently used theory worldwide for determining the torsional load-bearing

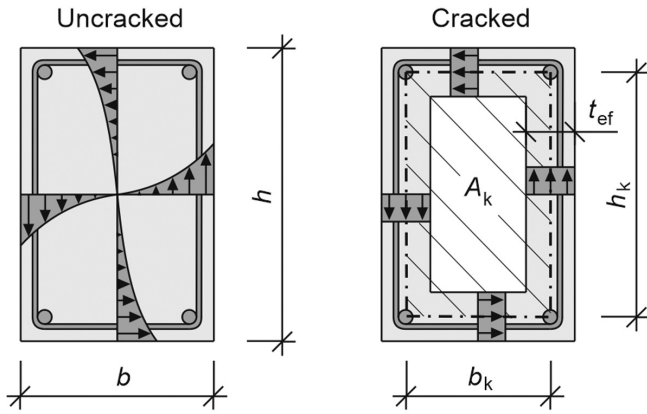


FIGURE 4 Fictitious thin-walled hollow cross-section of a solid cross-section under torsion

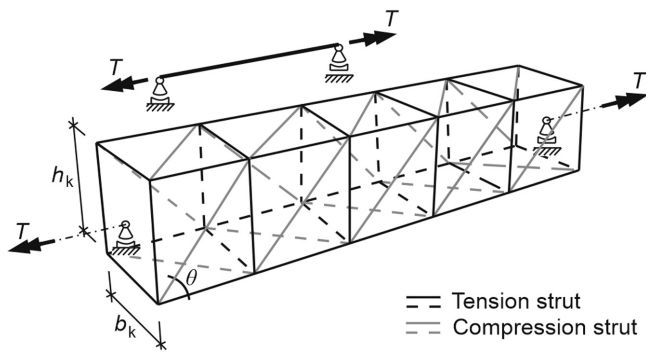


FIGURE 5 Space truss model for reinforced concrete beams

capacity, which was first developed by Rausch^{30,31} and refined by Lampert and Thürlimann,³² among others. For example, the refined form is included in DIN EN 1992-1-1/NAD^{5,6} (EC2/NAD) and Model Code 2010² (MC2010). In the refined space truss model, it is assumed that only the reinforced edge zones of the cross-section are available for torsional load transfer and, on the basis of this, solid and hollow cross-sections must be idealized to a fictitious thin-walled hollow cross-section with constant wall thickness t_{ef} . A constant shear flow

$$v = \frac{T}{2 \cdot A_k} \quad (1)$$

is assumed over the constant effective wall thickness t_{ef} according to Bredt's torsion theory^{33,34} (Figure 4). In Equation (1), T denotes the torsion moment and A_k the area within the center line of the fictitious thin-walled hollow cross-section, including inner hollow areas. Furthermore, the walls of the fictitious thin-walled hollow cross-section are idealized by a space truss model. The concrete compressive struts, inclined circumferentially at angle θ , are

in equilibrium with longitudinal and transverse tension struts consisting of longitudinal and transverse reinforcement (Figure 5). The longitudinal reinforcement is assumed to be concentrated in the corners, whereas the transverse reinforcement is thought to be concentrated in sections. The torsional load capacity is determined via the strut forces; shear stresses are not calculated. The strut forces can be determined from equilibrium observations on a truss node. To simplify matters, the unwinding of the fictitious thin-walled cross-section of a RC beam—the so-called shear wall model—is often considered (see References^{1,35}). With the shear wall model, the torsional load-bearing capacity of the longitudinal reinforcement results in

$$T_{sl} = \frac{A_{sl}}{u_k} \cdot f_{y,sl} \cdot 2 \cdot A_k \cdot \tan \theta, \quad (2)$$

and the torsional load-bearing capacity of the transverse reinforcement results in

$$T_{sw} = \frac{A_{sw}}{s_w} \cdot f_{y,sw} \cdot 2 \cdot A_k \cdot \cot \theta. \quad (3)$$

For the concrete compressive strut, however, the following applies

$$T_{cc} = \frac{k_c \cdot f_{cc} \cdot t_{ef} \cdot 2 \cdot A_k}{\cot \theta + \tan \theta}, \quad (4)$$

where A_{sl} is the cross sectional area of longitudinal reinforcement, A_{sw} is the cross sectional area of transverse reinforcement, $f_{y,sl}$ is the yield strength of longitudinal reinforcement, $f_{y,sw}$ is the yield strength of transverse reinforcement, f_{cc} is the concrete cylinder compressive strength, u_k is the perimeter of cross-section A_k , s_w is the spacing of the transverse reinforcement and k_c is the reduction factor of the concrete compressive strength.

The maximum supportable torsional moment of a RC beam results from the minimum of the load-bearing capacities of the individual struts according to Equation (2) to Equation (4) (compare also EC2/NAD and MC2010).

3.3 | Modified space truss model for SFR-RC beams

In order to take the load-bearing effect of the steel fibers into account, the (refined) space truss model must be modified. The steel fibers “suture” the cracks between the inclined concrete compressive struts and allow a force transmission across the cracks, so that this fiber load-bearing effect can be divided into a longitudinal and a

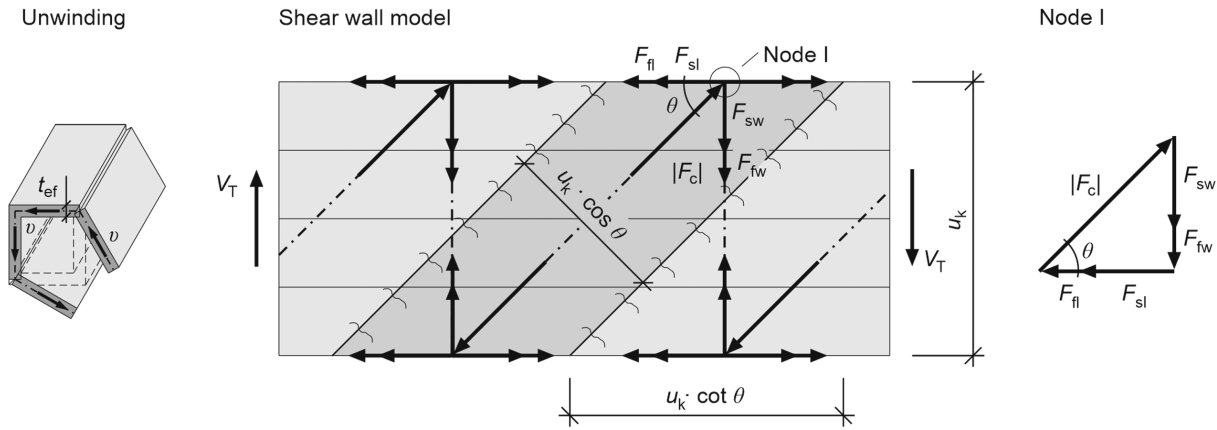


FIGURE 6 Unwinding (left), plane shear wall model (center), and force polygon for node I (right) of steel fiber reinforced RC beams (SFR-RC beams)

transverse part. If their load-bearing effect is understood as additional longitudinal and transverse tension struts, the shear wall model of a SFR-RC beam shown in Figure 6 results.¹ The additional strut forces F_{fl} and F_{fw} can be determined from equilibrium considerations at a truss node.

The shear flow v resulting from pure torsion (see Equation 1) can be summarized via the shear wall height u_k to a shear force V_T as follows:

$$V_T = v \cdot u_k = \frac{T \cdot u_k}{2 \cdot A_k} \quad (5)$$

The acting shear force is supported proportionally by the steel bars and the steel fibers in the longitudinal and transverse direction (cf. Reference¹). For the steel fiber tension struts in the longitudinal direction, the following thus applies

$$F_{fl} = V_T \cdot \cot \theta = \frac{T \cdot u_k \cdot \cot \theta}{2 \cdot A_k}, \quad (6)$$

and for the steel fiber struts in the transverse direction

$$F_{fw} = V_T = \frac{T \cdot u_k}{2 \cdot A_k} \quad (7)$$

If the strut forces are related to the corresponding (crack) surfaces, where

$$A_{fl} = u_k \cdot t_{ef}, \quad (8)$$

applies to the surface in the longitudinal direction and

$$A_{fw} = u_k \cdot \cot \theta \cdot t_{ef}, \quad (9)$$

applies to the surface in the transverse direction, the stress in the longitudinal direction can be determined as

$$\sigma_{fl} = \frac{F_{fl}}{A_{fl}} = \frac{T \cdot \cot \theta}{t_{ef} \cdot 2 \cdot A_k}, \quad (10)$$

and the stress in the transverse direction can be determined as

$$\sigma_{fw} = \frac{F_{fw}}{A_{fw}} = \frac{T}{\cot \theta \cdot t_{ef} \cdot 2 \cdot A_k}. \quad (11)$$

If Equations (10) and (11) are converted to T and the stresses are replaced by the respective post-crack tensile strength of the steel fiber concrete ($\sigma_{fl} = f_{ct,fl}$ and $\sigma_{fw} = f_{ct,fw}$), the torsional load capacities of the individual struts in the failure state can be determined. For the torsional strength of the steel fibers in the longitudinal direction

$$T_{fl} = f_{ct,fl} \cdot t_{ef} \cdot 2 \cdot A_k \cdot \tan \theta, \quad (12)$$

and for the torsional strength of the steel fibers in the transverse direction

$$T_{fw} = f_{ct,fw} \cdot t_{ef} \cdot 2 \cdot A_k \cdot \cot \theta, \quad (13)$$

results.

The torsional moment that can be supported in each direction is the sum of the torsional load-bearing capacity of the steel bars (Equations (2) and (3)) and the steel fibers (Equations (12) and (13)) in each direction. For the longitudinal direction this results in

$$T_{sfl} = T_{sl} + T_{fl}, \quad (14)$$

or

$$T_{\text{sfl}} = \frac{A_{\text{sl}}}{u_{\text{k}}} \cdot f_{\text{y,sl}} \cdot 2 \cdot A_{\text{k}} \cdot \tan\theta + f_{\text{ct,fl}} \cdot t_{\text{ef}} \cdot 2 \cdot A_{\text{k}} \cdot \tan\theta, \quad (15)$$

and for the transverse direction

$$T_{\text{sflw}} = T_{\text{sw}} + T_{\text{fw}}, \quad (16)$$

or

$$T_{\text{sflw}} = \frac{A_{\text{sw}}}{s_{\text{w}}} \cdot f_{\text{y,sw}} \cdot 2 \cdot A_{\text{k}} \cdot \cot\theta + f_{\text{ct,fw}} \cdot t_{\text{ef}} \cdot 2 \cdot A_{\text{k}} \cdot \cot\theta. \quad (17)$$

If there are no different post-crack tensile strengths of the steel fiber RC for the longitudinal and transverse directions (e.g., due to a specific alignment of the fibers³⁶), $f_{\text{ct,fl}} = f_{\text{ct,sw}}$ applies.

Since the concrete compressive strength is almost not influenced by the steel fibers (cf. e.g., MC2010²), Equation (4) applies to the concrete compressive strut. The maximum supportable torsional moment T_{R} of a SFR-RC beam results from the minimum of the load-bearing capacities of the tension struts T_{sfl} and T_{sflw} according to Equations (15) and (17) and the concrete compressive strut T_{cc} according to Equation (4):

$$T_{\text{R}} = \min \begin{cases} T_{\text{sfl}} \\ T_{\text{sflw}} \\ T_{\text{cc}} \end{cases} \quad (18)$$

4 | TORSION DATABASE “STEEL FIBRE REINFORCED CONCRETE”

4.1 | Selection criteria and data scope

To verify the prediction accuracy of the approach or the modified space truss model presented above (Equation (18)), the torsion database “Steel Fibre Reinforced Concrete” according to Reference¹ has been used, which includes a total of 269 torsional tests on concrete, RC and prestressed concrete beams made of normal strength fiber reinforced concrete (NSFR-RC) and ultra-high performance fiber reinforced concrete (UHPC) as well as reference tests from the international literature (torsional tests made of high performance fiber reinforced concrete [HPFRC] are currently not to be found in the literature). The reference tests are tests that have been carried out without steel fibers, but are otherwise identical in design to the fiber reinforced tests. With the

reference tests, the torsional load-bearing capacity of the steel fibers can be directly determined by comparison.

The following selection criteria were used to verify the approach:

- Minimum cross-section size of $b_{\text{m}} = \sqrt{h \cdot b} > 0.14 \text{ m}$ and $\min\{b; h\} \geq l_{\text{f}}/0.41$ (with l_{f} as length of the steel fibers),
- normal strength concretes ($12 \text{ N/mm}^2 \leq f_{\text{ck}} \leq 50 \text{ N/mm}^2$),
- macro fibers made of steel,
- ribbed steel reinforcing bars,
- RC beams with longitudinal and transverse reinforcement,
- one longitudinal reinforcement per corner of the transverse reinforcement and, if necessary, others distributed evenly over the length of the transverse reinforcement,
- longitudinal spacing of transverse reinforcement $s_{\text{w}} \leq h/2$ and
- torsional failure in the test (utilization of the torsional reinforcement or the concrete).

The minimum cross-sectional size was chosen so that, on the one hand, the space truss model can occur and, on the other hand, the steel fibers cannot extend over the entire (short) cross-sectional width and/or height due to their length and thus an extrapolation of the results obtained in the test to larger cross-sections must be questioned. The longitudinal spacing of the transverse reinforcement was chosen so that at least one transverse reinforcement crosses the torsion crack approximately in the middle and premature failure can be excluded. However, these criteria are not size effects.

Taking account of the selection criteria mentioned above, a total of 26 fiber reinforced tests and six reference tests without fiber reinforcement according to References^{17,28,29,37} remain. Consequently, it must be stated at this point that the experimental sampling is not very high, as no more suitable tests are currently documented in the literature. A summary of the selected tests is provided in Table 1 and further more information can be found in Reference.¹ Figure 7 shows the parameter range of the tests considered.

It becomes clear that, on the one hand, the investigated concrete compressive strengths f_{ck} (see Section 4.2.1) range from 17 to 52 N/mm² and thus the entire range of concrete compressive strengths of normal strength concrete is covered. On the other hand, the volumetric dosage of the fibers V_{f} varies between 0.3 and 1.5, the aspect ratio of the fibers λ between 37.5 and 75.0 (100.0), the longitudinal reinforcement ratio $\rho_{\text{sl}} = A_{\text{sl}}/(b \cdot h)$ between 0.5 and 1.6 and the stirrup reinforcement ratio $\rho_{\text{sw}} = (A_{\text{sw}}/s_{\text{w}} \cdot u_{\text{k}})/(b \cdot h)$ between 0.5 and 1.4, thus covering the usual ranges of construction practice.

TABLE 1 Properties of the used specimens (see also Ref.¹)

Ref.	Beam	b (mm)	h (mm)	t _{ef} (mm)	u _k (mm)	A _k (mm ²)	f _{ck} (N/mm ²)	f _{ctm,fl} (N/mm ²)	l _f (mm)	d _f (mm)	V _f (-)	f _{Ft,uk} (N/mm ²)	A _{sl} (cm ²)	ρ _{sl} (%)	f _{y,sl} (N/mm ²)	A _{sw} _{sw} (cm ² /m)	ρ _{sw} (%)	f _{y,sw} (N/mm ²)	T _{u,exp} (kNm)
17	T9	152.4	304.8	69.8	635.4	19,426.9	25.7	4.09	50.0	0.5	1.00	1.02	5.07	1.09	448.2	8.02	1.10	317.2	16.50
29	A-0.0	300.0	300.0	60.0	960.0	57,600.0	27.8	4.31	-	-	0.00	0.00	6.28	0.70	380.1	6.54	0.70	380.1	28.06
29	A-0.5	300.0	300.0	60.0	960.0	57,600.0	21.0	3.58	30.0	0.8	0.50	0.11	6.28	0.70	380.1	6.54	0.70	380.1	27.34
29	A-1.0	300.0	300.0	60.0	960.0	57,600.0	15.2	3.07	30.0	0.8	1.00	0.22	6.28	0.70	380.1	6.54	0.70	380.1	29.01
29	A-1.5	300.0	300.0	60.0	960.0	57,600.0	23.1	3.81	30.0	0.8	1.50	0.49	6.28	0.70	380.1	6.54	0.70	380.1	34.67
29	B-1.0	300.0	300.0	60.0	960.0	57,600.0	16.7	3.07	30.0	0.8	1.00	0.22	9.42	1.05	380.1	9.82	1.05	380.1	36.46
29	C-1.0	300.0	300.0	60.0	960.0	57,600.0	16.7	3.07	30.0	0.8	1.00	0.22	12.57	1.40	380.1	13.09	1.40	380.1	40.86
28	R40C-P	100.0	200.0	54.0	384.0	6716.0	35.7	5.10	-	-	0.00	0.00	2.01	1.01	432.0	5.59	1.07	432.0	5.52
28	R40C-F1	100.0	200.0	54.0	384.0	6716.0	36.1	5.13	41.0	0.5	0.30	0.19	2.01	1.01	432.0	5.59	1.07	432.0	5.56
28	R40C-F2	100.0	200.0	54.0	384.0	6716.0	37.1	5.23	41.0	0.5	0.60	0.41	2.01	1.01	432.0	5.59	1.07	432.0	5.69
28	R40C-F3	100.0	200.0	54.0	384.0	6716.0	38.0	5.31	41.0	0.5	0.90	0.67	2.01	1.01	432.0	5.59	1.07	432.0	5.73
28	R40C-F4	100.0	200.0	54.0	384.0	6716.0	39.3	5.43	41.0	0.5	1.20	0.97	2.01	1.01	432.0	5.59	1.07	432.0	5.82
28	R40L-P	100.0	200.0	52.0	392.0	7104.0	36.2	5.14	-	-	0.00	0.00	3.14	1.57	432.0	2.83	0.55	432.0	4.06
28	R40L-F1	100.0	200.0	52.0	392.0	7104.0	37.3	5.25	41.0	0.5	0.30	0.20	3.14	1.57	432.0	2.83	0.55	432.0	4.11
28	R40L-F2	100.0	200.0	52.0	392.0	7104.0	38.2	5.33	41.0	0.5	0.60	0.42	3.14	1.57	432.0	2.83	0.55	432.0	4.19
28	R40L-F3	100.0	200.0	52.0	392.0	7104.0	39.4	5.44	41.0	0.5	0.90	0.68	3.14	1.57	432.0	2.83	0.55	432.0	4.23
28	R40L-F4	100.0	200.0	52.0	392.0	7104.0	40.1	5.51	41.0	0.5	1.20	0.99	3.14	1.57	432.0	2.83	0.55	432.0	4.23
28	R40T-P	100.0	200.0	52.0	392.0	7104.0	36.2	5.15	-	-	0.00	0.00	1.13	0.57	432.0	5.03	0.99	432.0	3.76
28	R40T-F1	100.0	200.0	52.0	392.0	7104.0	37.5	5.27	41.0	0.5	0.30	0.20	1.13	0.57	432.0	5.03	0.99	432.0	3.85
28	R40T-F2	100.0	200.0	52.0	392.0	7104.0	38.8	5.39	41.0	0.5	0.60	0.43	1.13	0.57	432.0	5.03	0.99	432.0	3.93

(Continues)

TABLE 1 (Continued)

Ref.	Beam	b (mm)	h (mm)	t _{ef} (mm)	u _k (mm)	A _k (mm ²)	f _{ck} (N/mm ²)	f _{ctm,fl} (N/mm ²)	l _f (mm)	d _f (mm)	V _f (-)	f _{Ftuk} (N/mm ²)	A _{sl} (cm ²)	ρ _{sl} (%)	f _{y,sl} (N/mm ²)	A _{sw} / _{sw} (cm ² /m)	ρ _{sw} (%)	f _{y,sw} (N/mm ²)	T _{u,exp} (kNm)
28	R40T-F3	100.0	200.0	52.0	392.0	7104.0	39.1	5.41	41.0	0.5	0.90	0.68	1.13	0.57	432.0	5.03	0.99	432.0	3.98
28	R40T-F4	100.0	200.0	52.0	392.0	7104.0	39.9	5.49	41.0	0.5	1.20	0.98	1.13	0.57	432.0	5.03	0.99	432.0	4.02
37	R50C-P	100.0	200.0	56.0	376.0	6336.0	46.1	6.05	-	-	0.00	0.00	3.14	1.57	432.0	6.28	1.18	432.0	6.58
37	R50C-F1	100.0	200.0	56.0	376.0	6336.0	47.0	6.12	41.0	0.5	0.30	0.23	3.14	1.57	432.0	6.28	1.18	432.0	6.67
37	R50C-F2	100.0	200.0	56.0	376.0	6336.0	47.8	6.20	41.0	0.5	0.60	0.49	3.14	1.57	432.0	6.28	1.18	432.0	6.76
37	R50C-F3	100.0	200.0	56.0	376.0	6336.0	48.5	6.25	41.0	0.5	0.90	0.78	3.14	1.57	432.0	6.28	1.18	432.0	6.84
37	R50C-F4	100.0	200.0	56.0	376.0	6336.0	49.9	6.37	41.0	0.5	1.20	1.14	3.14	1.57	432.0	6.28	1.18	432.0	6.93
37	R50T-P	100.0	200.0	52.0	392.0	7104.0	47.4	6.15	-	-	0.00	0.00	1.13	0.57	432.0	6.28	1.23	432.0	5.69
37	R50T-F1	100.0	200.0	52.0	392.0	7104.0	48.6	6.27	41.0	0.5	0.30	0.24	1.13	0.57	432.0	6.28	1.23	432.0	5.77
37	R50T-F2	100.0	200.0	52.0	392.0	7104.0	49.2	6.31	41.0	0.5	0.60	0.50	1.13	0.57	432.0	6.28	1.23	432.0	5.82
37	R50T-F3	100.0	200.0	52.0	392.0	7104.0	50.1	6.18	41.0	0.5	0.90	0.77	1.13	0.57	432.0	6.28	1.23	432.0	5.90
37	R50T-F4	100.0	200.0	52.0	392.0	7104.0	51.5	6.25	41.0	0.5	1.20	1.12	1.13	0.57	432.0	6.28	1.23	432.0	5.99

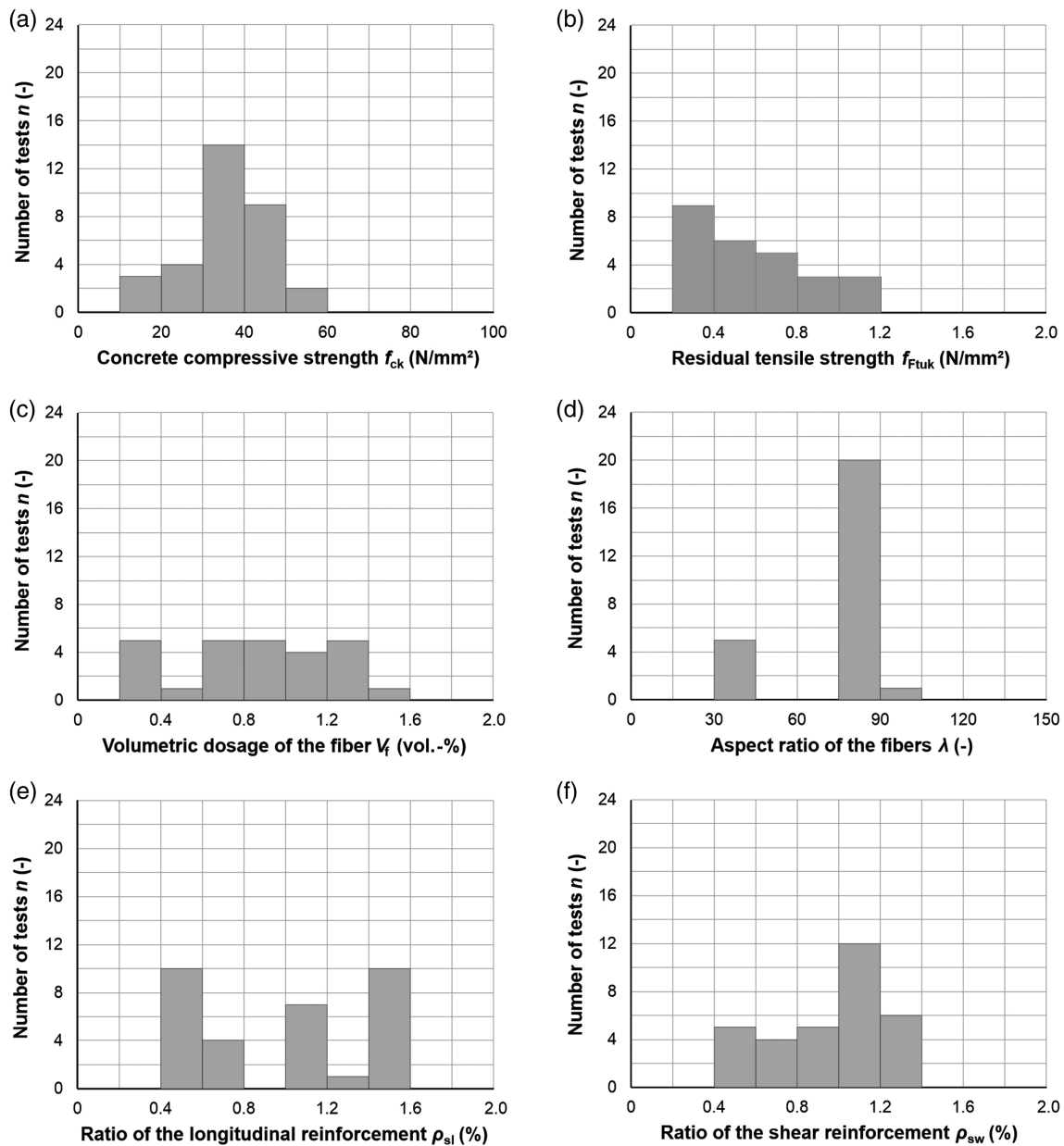


FIGURE 7 Range of parameters of the used data of the fiber reinforced tests with regard to (a) concrete compressive strength f_{ck} , (b) residual tensile strength of the concrete f_{ftuk} , (c) volumetric dosage of the fibers V_f , (d) aspect ratio of the fibers λ , (e) ratio of the longitudinal reinforcement ρ_{sl} , and (f) ratio of the transverse reinforcement ρ_{sw}

4.2 | Basis of evaluation and assumptions

4.2.1 | Concrete compressive strength of the (fibers reinforced) concrete

The characteristic value of the concrete compressive strength was determined according to Reference³⁸ for the evaluation of tests as follows:

$$f_{ck} = f_{cm} - 4.0 \text{ N/mm}^2, \quad (19)$$

where f_{cm} is the mean value of the cylinder compressive strength of the concrete (cylinder: $\varnothing/h = 150/300$ [mm]).

Since the concrete compressive strength is (almost) not influenced by the steel fibers, the strength reduction factor k_c according to MC2010 was applied in Equation (4) for the concrete compression strut:

$$k_c = k_e \cdot \eta_{fc}, \quad (20)$$

where k_e is the coefficient for the state of strain in the webs of beams ($k_e = 0.55$ for “level I approximation”) and η_{fc} is the coefficient for the effect of brittle failure

behavior of concrete of strengths greater than 30 N/mm² ($\eta_{fc} = (30/f_{ck})^{1/3} \leq 1.0$).

4.2.2 | Residual tensile strength of the fibers RC

Since the individual literature references only contain information on the splitting tensile strengths of the steel fiber RC used, the mean value of the residual post-crack flexural tensile strengths was determined using the empirical approach according to Reference¹¹ (for the estimation of the residual post-crack flexural tensile strengths of unnotched four-point bending tests, see Reference³⁹):

$$f_{Rim} = \frac{1}{0.37} \cdot k \cdot V_f \cdot (1 - k \cdot V_f) \cdot \frac{f_{ctm,fl}}{0.39} \cdot \zeta_{Li} \cdot \eta_V, \quad (21)$$

where k is the factor that depends on the type of fibers with $k = l_f/d_f \cdot \chi$ for steel wire fibers; χ is the factor that depends on the anchoring of the fiber with $\chi = 0.3$ for endhooked steel fibers and $\chi = 0.2$ for straight steel fibers; V_f is the volumetric dosage of the fibers [-]; $f_{ctm,fl}$ is the flexural tensile strength of the concrete according to MC2010² [N/mm²]; ζ_i is the coefficient for taking into account the fiber effect as a function of the length of the fibers and the CMOD considered with $\zeta_1 = 1.18 - \frac{7.5 \cdot l_f}{1000}$ for $CMOD_1 = 0.5$ mm and $\zeta_3 = 0.42 + \frac{7.5 \cdot l_f}{1000}$ for $CMOD_3 = 2.5$ mm; η_V is the coefficient for considering the nonlinear influence of the dosage of the fibers with $\eta_V = 1/(0.7 - 0.2 \cdot V_f)$.

The mean value of serviceability residual strength f_{Ftsm} and ultimate residual tensile strength f_{Ftum} were calculated according to MC2010 as follows:

$$f_{Ftsm} = 0.45 \cdot f_{R1m}, \quad (22)$$

$$f_{Ftum} = f_{Ftsm} - \frac{w_u}{CMOD_3} \cdot (f_{Ftsm} - 0.5 \cdot f_{R3m} + 0.2 \cdot f_{R1m}) \geq 0, \quad (23)$$

where w_u is the maximum crack opening accepted in structural design (depends on the ductility required) with $w_u = 1.5$ mm according to MC2010 and $CMOD_3$ is the crack mode opening displacement with $CMOD_3 = 2.5$ mm according to MC2010² or EN 14561.⁴⁰

As MC2010² does not contain any information on the determination of the characteristic value of the residual tensile strength, this is determined by means of a factor of 0.6 following Reference.⁴¹ Furthermore, according to MC2010, the fiber orientation must be taken into account. Since the torsional load-bearing behavior of

SFR-RC beams can be attributed to shear stresses, a fiber orientation factor of $K = 2.0$ was assumed following e. g. Reference.⁴² From this follows for the characteristic value of the ultimate residual tensile strength f_{Ftuk} :

$$f_{Ftuk} = \frac{0.60 \cdot f_{Ftu}}{2.0}. \quad (24)$$

This value was assumed for the longitudinal and transverse direction, so that in Equations (15) and (17) $f_{Ftuk} = f_{ct,fl} = f_{ct,sw}$ applies.

4.2.3 | Definition of the ideal hollow cross-section

According to MC2010, the effective wall thickness t_{ef} for solid cross-sections is defined as follows:

$$t_{ef} \leq d_k/8 \geq 2 \cdot (c_{nom,sw} + \phi_{sw} + \phi_{sl}/2), \quad (25)$$

where d_k is the diameter of the circle that might be inscribed at the most narrow part of the cross-section, $c_{nom,sw}$ is the nominal value of concrete cover of the transverse reinforcement, ϕ_{sw} is the diameter of the transverse reinforcement and ϕ_{sl} is the diameter of the longitudinal reinforcement.

5 | VERIFICATION OF THE MODIFIED SPACE TRUSS MODEL

5.1 | General

The evaluation of the torsion database “Steel Fibre Reinforced Concrete” was carried out as follows:

- The model safety factor is defined as $\gamma_{mod} = T_{u,exp}/T_{u,cal,k}$ and in order to satisfy the safety requirements for the design, the percentage of tests with $\gamma_{mod} < 1.0$ must be less than 5%.
- The value $T_{u,exp}$ is the torsional failure load measured in the test.
- The value $T_{u,cal,k}$ refers to the calculated characteristic torsional load capacity (Equation 18) of the test.
- The yield strength of the longitudinal reinforcement $f_{y,sl}$ and the yield strength of the transverse reinforcement $f_{y,sw}$ were assumed without the partial safety factor γ_s for the material properties of reinforcing steel.
- The characteristic concrete compressive strength f_{ck} was assumed without taking the factors β_{cc} and $\beta_{c,sus}$ for time effects as well as without the partial safety factor γ_c for concrete material properties into account.

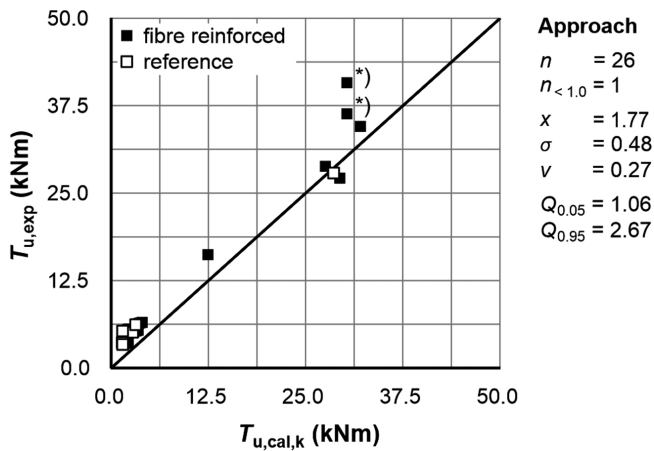


FIGURE 8 Comparison of the experimental and calculated torsional moments

- The characteristic value of the ultimate residual tensile strength $f_{Ftu,k}$ was assumed without the partial safety factor γ_F for fiber RC.

In order to validate the approach, the experimental values $T_{u,exp}$ are compared with the calculated characteristic values $T_{u,cal,k}$ of the torsional moment. The statistical parameters listed were determined from the model safety coefficient $\gamma_{mod} = T_{u,exp} / T_{u,cal,k}$ assuming a standard normal distribution, n is the number of tests, $n_{<1.0}$ is the number of tests with $\gamma_{mod} < 1.0$, x is the mean value, σ is the standard deviation, ν is the variation coefficient and $Q_{0.05;0.95}$ is the 5%-; 95%- quantile.

5.2 | Evaluation

Figure 8 shows the comparison of the experimental and calculated torsional moments. A distinction is made between SFR-RC tests (fiber reinforced) and reference RC tests without steel fibers (reference).

The evaluation shows that the approach (see Section 3.3) provides good to very good agreement with the experimental values. Only one test cannot be recalculated so well. This is a test with a calculated failure of the concrete compressive strut (T_{cc} according to Equation 4), which is marked with an “(*)” in Figure 8. However, it should be noted here that the results are based on “only” 26 tests and are thus somewhat limited, as no more suitable tests are currently documented in the literature (see also Section 4.1).

Figure 9 shows the influence of significant model parameters on the model safety factor γ_{mod} and on the prediction accuracy of the approach.

For the concrete compressive strength f_{ck} it becomes clear that the entire range of MC2010 is covered with regard to the concrete compressive strength classes for

normal strength concrete, and that with the increasing of the concrete compressive strength the model safety factor γ_{mod} increases, and thus, the calculated value increasingly underestimates the experimental value.

With regard to the characteristic value of the ultimate residual tensile strength $f_{Ftu,k}$ and the volumetric dosage of the fibers V_f , it can be seen that, on the one hand, lower scatter occurs with increasing ultimate residual tensile strength or with increasing volumetric dosage of the fibers and, on the other hand, the reference tests without steel fibers show the greatest scatter. Consequently, the approach proposed according to Section 3.3 (modified space truss model) for SFR-RC torsion tests achieves slightly better agreements between experimental and calculated torsional moments than the calculation approach according to Section 3.2 or MC2010 (refined space truss model) for pure RC torsion tests (without steel fibers). Additionally, it is shown that the tests considered, cover the entire range of the usual performance of steel fiber concrete (characteristic value of the ultimate residual tensile strength $f_{Ftu,k}$ according to MC20210).

The evaluations for the model parameters middle cross-section size b_m , longitudinal reinforcement ratio ρ_{sl} and transverse reinforcement ratio ρ_{sw} do not reveal any real trend. With regard to the model parameters middle cross-section size b_m , it must be noted that so far only small cross-sections have been investigated. For this reason, no conclusions can be made about any kind of size effects, as occurs, for example, with beams under shear loading (cf. References^{38,42}). It must also be mentioned that no size effects occur with RC beams under torsional loads (among other things due to the clear load transfer and the missing crack stresses) (cf. References³⁵). However, the tests considered here cover the usual ratios of longitudinal and transverse reinforcement in practice.

In principle, the approach (modified space truss model) provides model safety factors above 1.0. Only one fiber reinforced test (fiber reinforced) and one reference test without steel fibers (reference) are just below 1.0, which means that the proportion of steel fiber reinforced tests with $\gamma_{mod} < 1.0$ is less than 5%, so that the safety requirements for a design are achieved. The mean value is 1.77 (experimental values $T_{u,exp}$ compared with calculated characteristic values $T_{u,cal,k}$) and is thus comparable to other models for steel fiber RC or RC under shear loading (e.g., References^{2,5,38,43}).

Figure 10 shows an evaluation of the torsional strength of the steel fibers in the longitudinal direction (Equation 12) and in the transverse direction (Equation 13) in relation to the total torsional moment of the longitudinal direction (Equation 14) and of the transverse direction (Equation 16). It can be seen that in the tests considered, the torsional load-bearing capacity of

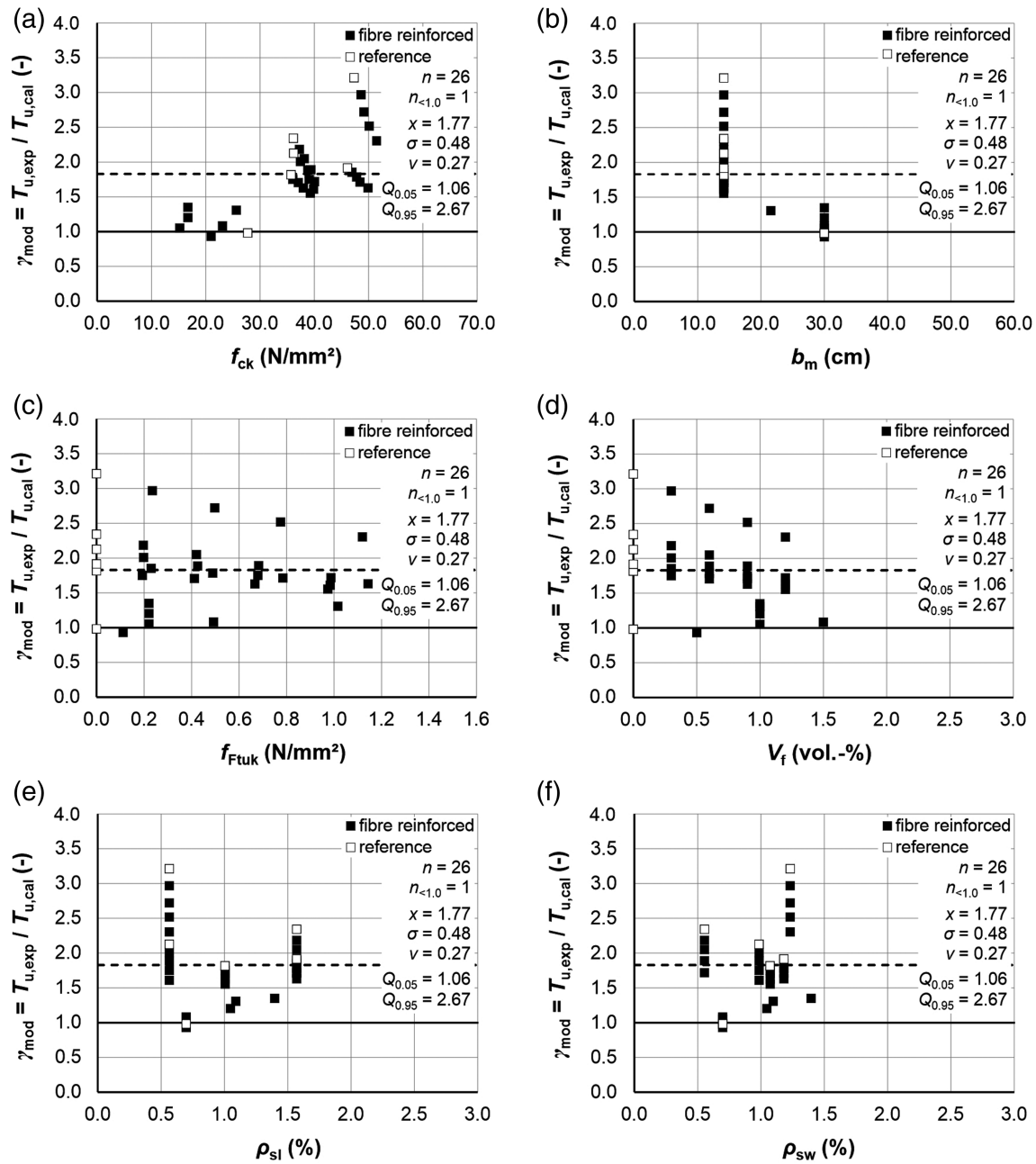


FIGURE 9 Model safety factor γ_{mod} as a function of: (a) the characteristic value of the concrete compressive strength f_{ck} , (b) the middle cross-section size b_m , (c) the characteristic value of the ultimate residual tensile strength f_{ftuk} , (d) the volumetric dosage of the fibers V_f , (e) the ratio of the longitudinal reinforcement ρ_{sl} , and (f) the ratio of the transverse reinforcement ρ_{sw}

the fibers is up to about 30% and therefore it makes sense to take the fiber load-bearing effect into account in the torsional design.

6 | SUMMARY AND CONCLUSIONS

The use of steel fibers increases the load capacity and robustness of beams under pure torsion. This increase

depends on the dosage and the performance of the steel fibers.

In the case of SFRC beams, only a slight increase in the torsional cracking or ultimate torsional moment can be observed. In the post-cracking phase of the torque-twist curve, however, a significant influence can be noticed.

SFRC beams that are additionally reinforced with longitudinal reinforcement or with transverse reinforcement show a more ductile load-bearing behavior, but the

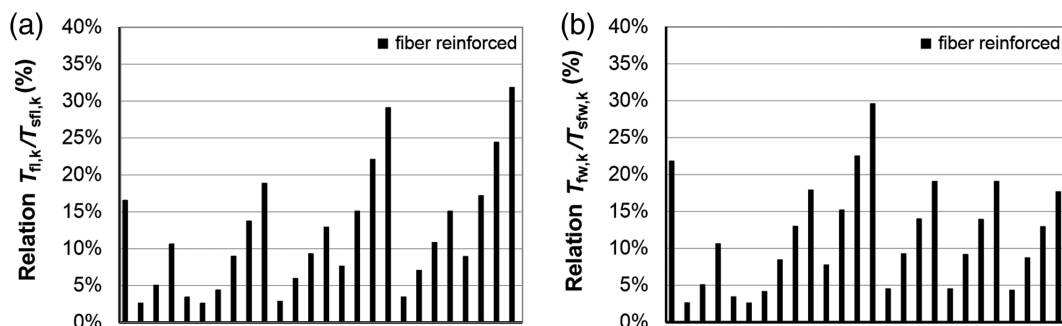


FIGURE 10 Calculated torsional strength of the steel fibers (Equations 12 and 13) in relation to the total torsional moment (Equations 14 and 16): (a) longitudinal direction and (b) transverse direction

longitudinal or transverse reinforcement is not utilized. The ultimate torsional moment is only marginally increased by the steel fibers; an increase in the degree of longitudinal or transverse reinforcement, on the other hand, does not increase the ultimate torsional moment. Consequently, the design of fiber RC beams with longitudinal or transverse reinforcement does not make sense, as the steel fibers cannot completely replace a missing longitudinal and/or transverse reinforcement.

A significant improvement of the torque-twist response can only be achieved with steel fiber reinforced beams with longitudinal reinforcement and transverse reinforcement (SFR-RC beams). In this case, a slightly higher torsional cracking moment, a finer crack pattern, a higher torsional stiffness after cracking and a higher ultimate torsional moment occur due to the steel fibers, which is why a consideration of the load-bearing effect of the steel fibers in the torsional design of SFR-RC beams seems appropriate.

Based on this, the well-known space truss model for RC beams was extended to include the load-bearing effect of the steel fibers. For this purpose, the steel fiber load-bearing effect was understood as additional tension struts in longitudinal and transverse direction and an additive approach was proposed (modified space truss model (Figure 6), Equation 18). The modified space truss model was checked with the help of torsion database “Steel Fibre Reinforced Concrete” according to Reference,¹ which was filtered with regard to SFR-RC beams made of normal strength concrete with macro fibers. The evaluations show that good to very good agreements with experimental torsional moments are achieved with this model and that the safety requirements with regard to a design are complied. In addition, the evaluation shows that in the tests considered here, the (calculated) load-bearing capacity of the fibers can amount to up to 30% of the torsional failure moment (Figure 10). However, it should be noted that the experimental sampling is not very high (26 tests) and the results are therefore somewhat limited.

The tests considered cover the entire application range of MC2010 for normal strength fiber reinforced concrete (NSFRC) and the parameters commonly used in practice. When using the approach, however, the limits according to Section 4.1 must be considered and it must be taken into account that the mean cross-section size b_m studied was (only) between 14 and 30, it is pointed out that large-scale tests should be conducted to verify the adequacy of the proposed modified space truss model here. In addition, the literature does not currently contain any torsion tests on SFR-RC beams made of high-performance fiber reinforced concrete (HPFRC). However, an approach for UHPFRC can be taken from References.^{1,27}

ACKNOWLEDGMENT

Open Access funding enabled and organized by Projekt DEAL.

DATA AVAILABILITY STATEMENT

The data that support the findings of this study are available from the corresponding author upon reasonable request.

ORCID

Vincent Oettel  <https://orcid.org/0000-0003-4206-5622>

REFERENCES

- Oettel V. V. Torsionstragverhalten von stahlfaserbewehrten Beton-, Stahlbeton- und Spannbetonbalken [Doctoral thesis]. Braunschweig: Technische Universität Braunschweig; 2016. <https://doi.org/10.24355/dbbs.084-201606210916-0>
- fib – Fédération Internationale du Béton. *fib* model code for concrete structures 2010. Berlin: Ernst & Sohn; 2013.
- Oettel V, Empelmann M. Monolithische Balken und vorgespannte Segmentbauteile aus UHPC unter Torsions- und kombinierter Biege-, Querkraft- und Torsionsbeanspruchung. Zwischenkolloquium DFG-Schwerpunktprogramm 1182 “Nachhaltiges Bauen mit UHPC”, Kassel. 2011.

4. Oettel V. Faserbeton unter Torsionsbeanspruchung. Proceedings of 1. DAfStb-Jahrestagung mit 54. Bochum: DAfStb-Forschungskolloquium; 2013. p. 315–20.
5. DIN EN 1992-1-1. Eurocode 2: Design of concrete structures – Part 1-1: General rules and rules for buildings. Berlin: Beuth Verlag; 2011.
6. DIN EN 1992-1-1. Eurocode 2: Design of concrete structures – Part 1-1: General rules and rules for buildings - National Annex Germany. Berlin: Beuth Verlag; 2013.
7. Mark P, Oettel V, Look K, Empelmann M. Neuauflage DAfStb-Richtlinie Stahlfaserbeton. Beton- und Stahlbetonbau. 2021; 116:19–25. <https://doi.org/10.1002/best.202000065>
8. Heek P, Look K, Oettel V, Mark P. Bemessung von Stahlfaserbeton und stahlfaserbewehrtem Stahlbeton. Beton- und Stahlbetonbau. 2021;112:2–12. <https://doi.org/10.1002/best.202100009>
9. Amin A, Bentz EC. Strength of steel fiber reinforced concrete beams in pure torsion. Struct Concr. 2018;19:684–94.
10. Deifalla AF, Zapris AG, Chalioris CE. Multivariable regression strength model for steel fiber-reinforced concrete beams under torsion. Materials. 2021;14:3889. <https://doi.org/10.3390/ma14143889>
11. Oettel V, Schulz M, Haist M. Empirical approach for the residual flexural tensile strength of steel fiber reinforced concrete based on notched three-point bending tests. Struct Concr. 2022; 23:993–1004. <https://doi.org/10.1002/SUCO.202100565>
12. Hafeez Khan TA, Sanjeeva Reddy T, Sadananda Murthy P. An experimental study of fibre-reinforced concrete beams under pure torsion. Indian Concr J. 1976;50:314–7.
13. Narayanan R, Toorani-Goloosalar Z. Fibre reinforced concrete in pure torsion and in combined bending and torsion. Proc Inst Civil Eng. 1979;2:987–1001.
14. Facconi L, Minelli F, Ceresa P, Plizzari G. Steel fibers for replacing minimum reinforcement in beams under torsion. Mater Struct. 2021;54:34. <https://doi.org/10.1617/s11527-021-01615-y>
15. Wafa FW, Hasnat A, Tarabolsi OF. Prestressed fiber reinforced concrete beams subjected to torsion. ACI Struct J. 1992;89(3): 272–83.
16. Leonhardt F, Schelling G. Torsionsversuche an Stahlbetonbalken. Deutscher Ausschuss für Stahlbeton (DAfStb), Issue 239. Berlin, Germany: Ernst und Sohn Verlag; 1974.
17. Craig RJR, Dunya S, Riaz J, Shirazi H. Torsional behavior of reinforced fibrous concrete beams. ACI Special Pub. 1984;81: 17–49.
18. Chalioris CE, Karayannis CG. Effectiveness of the use of steel fibres on the torsional behaviour of flanged concrete beams. Cem Concr Compos. 2009;31:331–41. <https://doi.org/10.1016/j.cemconcomp.2009.02.007>
19. Mansur MA, Lim TY. Torsional behaviour of reinforced fibre concrete beams. Int J Cem Compos Lightweight Concr. 1985;7: 261–7.
20. Rao GTD, Seshu RD. Torsion of steel fiber reinforced concrete members. Cem Concr Res. 2003;33:1783–8. [https://doi.org/10.1016/S0008-8846\(03\)00174-1](https://doi.org/10.1016/S0008-8846(03)00174-1)
21. Craig RJR, Parr JA, Germain E, Mosquera V, Kamilaris S. Fiber reinforced beams in torsion. ACI J. 1986;83:934–42.
22. Joh C, Lee J, Yang I-H, Kim, B-S. Torsional test of ultra high performance fiber-reinforced concrete square members. Proceedings of 3rd International Symposium on UHPC and Nanotechnology for High Performance Construction Materials, Kassel. p. 509–516.
23. Bach C, Graf O. Versuche über die Widerstandsfähigkeit von Beton und Eisenbeton gegen Verdrehung. Deutscher Ausschuss für Eisenbeton, Issue 16. Berlin: Ernst und Sohn Verlag; 1912.
24. Yang I-H, Joh C, Lee JW, Kim B-S. Torsional behavior of ultra-high performance concrete squared beams. Eng Struct. 2013; 56:372–83. <https://doi.org/10.1016/j.engstruct.2013.05.027>
25. Rao GTD, Seshu RD. Torsional response of fibrous reinforced concrete members: effect of single type of reinforcement. Construct Build Mater. 2006;20:187–92. <https://doi.org/10.1016/j.conbuildmat.2005.01.017>
26. Ismail M. Behavior of UHPC structural members subjected to pure torsion. [Doctoral thesis]. Kassel: Universität Kassel; 2015. Available from: <https://d-nb.info/1080266399/34>
27. Oettel V, Empelmann M. Monolithic box girders and prestressed segmental components made of UHPC under torsion and combined bending, shear and torsion. Sustainable building with ultra-high performance concrete. Kassel: Uni Press Kassel; 2014. p. 515–30.
28. Rao GTD, Seshu RD. Analytical model for the torsional response of steel fiber reinforced concrete members under pure torsion. Cem Concr Compos. 2005;27:493–501. <https://doi.org/10.1016/j.cemconcomp.2004.03.006>
29. Mansur MA, Nagataki S, Lee SH, Oosumimoto Y. Torsional response of reinforced fibrous concrete beams. ACI Struct J. 1989;86(1):36–44.
30. Rausch E. Berechnung des Eisenbetons gegen Verdrehung (Torsion) und Abscheren. Berlin, Germany: Verlag von Julius Springer; 1929.
31. Rausch E. Drillung (Torsion), Schub und Scheren im Stahlbetonbau. 3rd ed. Düsseldorf, Germany: Deutscher Ingenieur-Verlag; 1953.
32. Lampert P, Thürlimann B. Torsionsversuche an Stahlbetonbalken. Zürich: Institut für Baustatik ETH Zürich; 1968 Report No. 6506-2.
33. Bredt R. Kritische Bemerkungen zur Drehungselastizität. Zeitschrift des Vereins Deutscher Ingenieure. 1896;40(28):785–90.
34. Bredt R. Kritische Bemerkungen zur Drehungselastizität. Zeitschrift des Vereins Deutscher Ingenieure. 1896;40(29):813–7.
35. Zedler T. Zum Tragverhalten von Stahlbeton- und Spannbetonbalken unter Torsion. [Doctoral thesis]. Bochum: Ruhr Universität Bochum; 2011. Available from: <https://hss-opus.ub.ruhr-uni-bochum.de/opus4/frontdoor/deliver/index/docId/2740/file/diss.pdf>
36. Mu R, Li H, Qing L, Lin J, Zhao Q. Aligning steel fibers in cement mortar using electro-magnetic field. Construct Build Mater. 2017;131:309–16. <https://doi.org/10.1016/j.conbuildmat.2016.11.081>
37. Rao GTD, Seshu RD, Warnitchai P. Effect of steel fibers on the behaviour of over-reinforced beams subjected to pure torsion. Civil Eng Dimens. 2010;12(1):44–51.
38. Reineck K-H, Kuchma DA, Fitik B. Extended databases with shear tests in structural concrete beams without and with stirrups for the assessment of shear design procedures. Research Report. 2010.
39. Oettel V, Schulz M, Lanwer J-P. Empirischer Ansatz zur Bestimmung der Nachrissbiegezugfestigkeit. Beton- und

- Stahlbetonbau. 2021;112:24–35. <https://doi.org/10.1002/best.202100002>
40. EN 14651. Test method for metallic fibre concrete - Measuring the flexural tensile strength (limit or proportionality (LOP), residual). Brussels, Belgium: European Committee for Standardization (CEN); 2005.
41. Look K, Landler J, Mark P, Fischer O. Fasermengen und Leistungsklassen. Beton- und Stahlbetonbau. 2021;112:13–23. <https://doi.org/10.1002/best.202100004>
42. Rosenbusch J. Zur Querkrafttragfähigkeit von Balken aus stahlfaserverstärktem Stahlbeton. [Doctoral thesis]. Braunschweig: Technische Universität Braunschweig; 2003. <https://doi.org/10.24355/dbbs.084-200511080100-519>
43. Mantelli SG, Faconi L, Look K, Medeghini F, Mark P, Minelli F, et al. Code provisions for shear strength in prestressed FRC members: a critical review. In: Serna P, Llano-Torre A, Martí-Vargas JR, Navarro-Gregori J, editors. Fibre reinforced concrete: improvements and innovations II. BEFIB 2021. RILEM Bookseries, vol 36. Cham: Springer; 2022. https://doi.org/10.1007/978-3-030-83719-8_50

AUTHOR BIOGRAPHY



Vincent Oettel, Professor and Head of Institute, Institute of Concrete Construction (IfMa), Leibniz Universität Hannover, Appelstraße 9A, 30167 Hannover, Germany.

Email: oettel@ifma.uni-hannover.de

How to cite this article: Oettel V. Steel fiber reinforced RC beams in pure torsion—Load-bearing behavior and modified space truss model. *Structural Concrete*. 2023;24(1):1348–63. <https://doi.org/10.1002/suco.202200031>